ARTICLES

Extended Light Scattering Investigations on Dihydroxy Bile Salt Micelles in Low-Salt Aqueous Solutions

Martin Janich,* Jens Lange, and Heinrich Graener

Department of Physics/Optics, Martin-Luther-University Halle, 06099 Halle, Germany

Reinhard Neubert

Department of Pharmacy, Martin-Luther-University Halle, 06099 Halle, Germany

Received: December 17, 1997; In Final Form: March 25, 1998

Extended static and dynamic light scattering results on micellar solutions of the dihydroxy bile salt NaGDC (sodium glycodeoxycholate) are presented. From the measurements the apparent molar mass and the mean aggregation number, the apparent diffusion coefficient and the mean hydrodynamic radius for the micelles as a function of NaGDC concentration (8.5−28.0 g/L), ionic strength of the solution (0.03−0.2 M NaCl added), and temperature (20−35 °C) are deduced. The apparent micellar size versus surfactant concentration is discussed only in the context of intermicellar interactions. Growth processes are not taken into account. A self-consistent calculation of the concentration dependence of the diffusion coefficient very similar to that of Dorshow et al.[1,2] is applied in order to determine the potential of the micelles using the DLVO theory. The fractional ionization of the micelle surface is estimated. Moreover, the expansion of the analysis from Dorshow et al. shows that Hamaker's constant is proportional to the mean molar mass of the micelles.

Introduction

Many artificial and biological molecules are amphiphiles; that is, they consist of hydrophilic (ionic head groups or nonionic hydroxyl groups) and hydrophobic parts (hydrocarbon chains). Such molecules form micelles in polar solvents like water.[3] The most investigated simple amphiphiles, such as ethyltrimethylammonium salts or sodium dodecyl sulfate, consist only of one polar and one nonpolar part.[1−7] However, biological amphiphiles like the bile acids are more complex. They are composed of more than one polar group—one ionic and some hydroxyl groups—and a stiff nonpolar hydrocarbon skeleton (Figure 1).[8,9]

The determination of typical parameters of bile salt micelles such as size, aggregation number, and fractional ionization is a subject of considerable interest again.[10−12] This is because of the fact that natural micellar systems can be used as "carrier systems" for highly hydrophilic drug molecules.[12] Neutron and light scattering measurements are well-established methods for the investigation of small particles in solution and the determination of micellar parameters.[1−11,13−15] This article presents results from static and dynamic light scattering experiments on bile salt micelles. Using standard methods[16] both molar mass and diffusion coefficient can be determined from the mean scattered intensity and fluctuation of the scattered intensity. It turned out that both quantities vary monotonically with increasing bile salt concentration. Changing the ionic strength of the solution by adding NaCl, the slopes of the curves of the aggregation number or the diffusion coefficient versus surfactant concentration vary from positive to negative. This behavior is known from other ionic micelles, too.[1,2,4,7] As this variation of micellar parameters is an effect of both real change of size and change of interparticle interactions, the parameters are called "apparent". Some representative plots of such apparent quantities as a function of bile salt concentration and NaCl molarity are shown for the inverse molar mass and mean diffusivity, respectively (Figures 2, 3).

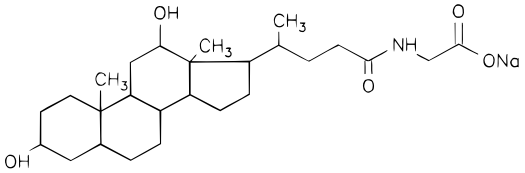

Figure 1. Structural formula of sodium glycodeoxycholate (NaGDC).

In the low-salt region ($c_{NaCl} < 0.2$ M) the slopes are positive and the curves are nearly linear. In the high-salt region the slopes are negative and the curves are clearly bended, an observation that is usually connected with an extensive micellar growth with increase of the bile salt concentration. This paper will discuss results only for low-salt concentrations.

In contrast to similar plots of simple surfactants, for bile salt micelles the intersections of the lines, which are related to the real inverse molar masses or diffusivities, depend on the NaCl concentrations.[1,2,4] This can be explained by a micellar growth increasing ionic strength,[8,17] which is not observed for simple surfactants. But the increase of the inverse apparent molar mass or the apparent micellar diffusivity with bile salt concentration is mainly an effect not caused by micellar growth. It can be explained by long-range interparticle interactions. The micelles exert forces on each other through a particle potential consisting

S1089-5647(98)00546-X CCC: $15.00
Published on Web 07/10/1998

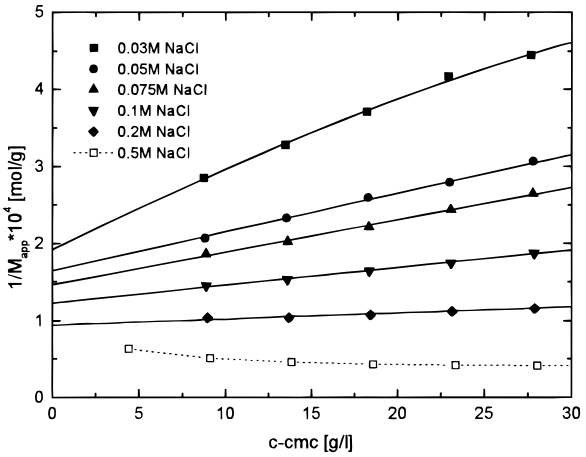

Figure 2. Inverse apparent molar masses of NaGDC micelles in aqueous solutions of different ionic strength at 25 °C. The symbols represent the experimental values, the solid lines simple second-order least-squares fits. The dotted line is a simple connection between data points to guide the eyes.

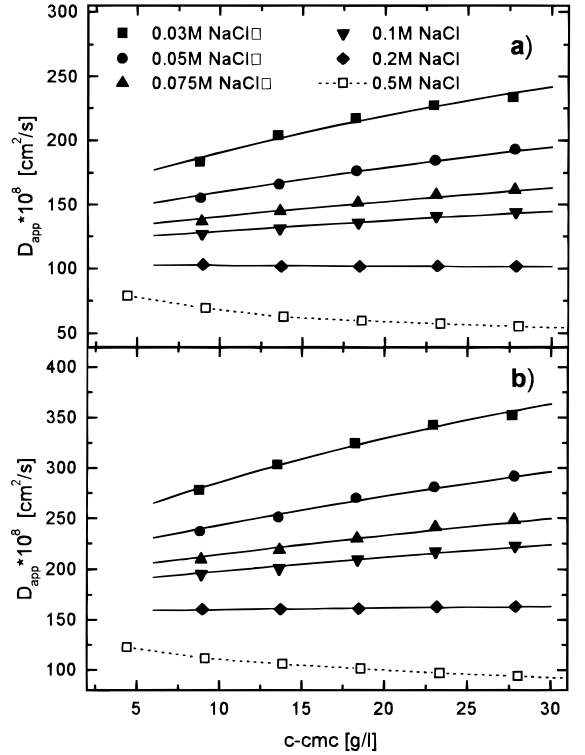

Figure 3. Apparent diffusion coefficients of NaGDC micelles in aqueous solutions of different ionic strength at (a) 20 °C and (b) 35 °C. The symbols represent the experimental values; the lines are fitted with the described theory. The dotted line is a simple connection between data points to guide the eyes.

of attractive and repulsive parts. Additionally, taking into account hydrodynamic interactions between micelles, which arise from the response of the solvent to stochastic motion of one particle in the neighborhood of others, one can explain the micellar diffusivities. In the low-salt regime, the long-range repulsive Coulomb potential is the main part of the interaction; as its screening is weak, coagulation of the particles is impossible because of the strong separation of each micelle. This separation causes formation of intermicellar structures in the solution. In scattering experiments these structures lead to destructive interference of the scattered intensity and therefore, using simple standard analysis methods, to variations of the molar mass. In addition, the intermicellar interactions impede the diffusion of the particles and thus the fluctuations of the scattered intensity, therefore resulting in the variation of the diffusion coefficients.

Article Survey. The next section gives a survey of the theory, which explains the behavior of the observed variation of micellar parameters in the low-salt regime mentioned above. Some formulas, similar to those which have been used in previous papers,[1,2,4,7] are briefly derived from basic calculations, and necessary extensions for the analysis of more complex surfactant systems are made. The limitation due to some approximations such as the linear expansion,[1,2,7] the use of the simple dilute gas part of the pair distribution function $g(r)$,[18,19] and the implementation of the DLVO potential[20] will be discussed. Next the idea of our fit routine, which is an expansion of that introduced by Dorshow et al.,[1,2] allowing the diffusion coefficient to vary with NaCl concentration, is introduced. Then sample preparation, experimental setup, and data acquisition are explained. Finally, the results are presented and discussed.

Theory

Dorshow et al.[1,2] have described a fit procedure for micellar diffusivities of simple surfactant micelles in low-salt solutions. They used a linear interaction theory as previously proposed by Corti and Degiorgio,[4] which takes into account a pair interaction potential from the DLVO theory of colloid stability[20] and a hydrodynamic correction from Felderhof.[21] His fit procedure requires two independent parameters, the degree of ionization α and the Hamaker coefficient A. This procedure cannot explain the micellar growth with increasing ionic strength. In this paper, an extended fit procedure for the micellar diffusivities using a third parameter and additionally simple quadratic least-squares fits for the inverse molar masses are presented. Our routine uses the independent adjustable parameters degree of ionization α, Hamaker's coefficient A, and additionally the free diffusion coefficient D_0.

Survey of Theory. The results of static and dynamic light scattering experiments on very small (*diameter* ≪ *wavelength of light*) but interacting particles in solution yield the apparent molar mass M_{app} and diffusion coefficient $D_{app,}$ respectively. Both are functions of the concentration and interparticle interactions. They are related to the real molar mass M_0 and the diffusion coefficient without interactions D_0 by the following equations.[7,18]

$$\frac{1}{M_{app}} = \frac{1}{M_0 S(q)} \tag{1}$$

$$D_{app} = \frac{D_0}{S(q)}\{1 + n(\delta_O + \delta_D + \delta_A + \delta_S)\} \tag{2}$$

where n is the number particle density, $S(q)$ is the structure factor, and δ_i are complicated functions of the scattering vector q, given by

$$\delta_O = 6\pi a \int_0^\infty dr\, r[g(r) - 1]\left\{\frac{\sin qr}{qr} + \frac{\cos qr}{(qr)^2} - \frac{\sin qr}{(qr)^3}\right\} \tag{3}$$

$$\delta_D = 4\pi a^3 \int_0^\infty \frac{dr}{r}[g(r) - 1]J_2(qr) + \frac{4\pi a^3}{3} \tag{4}$$

$$\delta_A = 4\pi\int_0^\infty dr\, r^2 g(r)\left\{\frac{9a^6}{8r^6} - \frac{5a^4}{4r^4}\right\} \quad (5)$$

$$\delta_S = 75\pi a^7 \int_0^\infty \frac{dr}{r^5} g(r)\left\{\frac{\sin qr}{qr} + \frac{2\cos qr}{(qr)^2} - \frac{2\sin qr}{(qr)^3}\right\} \quad (6)$$

The physical meaning of subscripts O, D, A, S is explained in detail in refs 18 and 21.

Apart from the correction term at the numerator linear to n both eqs 1 and 2 appear similar. Since the correction term is related to the hydrodynamic interactions, it is absent in the equation for the static light scattering measurement. Additionally, the structure factor $S(q)$ is also related to the pair distribution function $g(r)$. For isotropic systems the relation is given by[19]

$$S(q) = 1 + 4\pi n\int_0^\infty dr\, r^2[g(r) - 1]\frac{\sin qr}{qr} \quad (7)$$

$a = k_B T/6\pi\eta D_0$ is the hydrodynamic radius of the particles, T the temperature, k_B Boltzmann's constant, η the solvent viscosity, and J_2 the second-order Bessel function.

In general, the pair distribution function $g(r)$ is unknown.[19] However, for dilute gases it is simply $g(r) = \exp[V(r)/k_B T]$, where $V(r)$ is the interaction potential between the particles. For very dilute solutions this distribution function can be used as well. The potential is modeled in the following way:

$$V(r) = V_{hs} + V_{attr} + V_{rep} \quad (8)$$

V_{hs} is the hard sphere contribution, V_{attr} is the attractive part (dispersion forces), and V_{rep} is the repulsive electrostatic part. The first term of the potential, V_{hs}, is zero for $r > a$ and otherwise infinite. The next two parts will be discussed later as the well-known DLVO potential.

As in the case of light scattering, the scattering vector q is very small compared to the inverse of the size of the micelles; it is possible to reduce the formulas to the case of $q \to 0$. Replacing $r = 2a(x + 1)$ and integrating over the hard sphere contribution in $g(r)$, one gets

$$\frac{1}{M_{app}} = \frac{1}{M_0(1 - K_i\phi)} \approx \frac{1}{M_0}(1 + K_i\phi + ...) \qquad K_i\phi \ll 1 \quad (9)$$

$$D_{app} = D_0\frac{1 + K_h\phi}{1 - K_i\phi} \approx D_0[1 + (K_h + K_i)\phi + ...] \qquad K_i\phi \ll 1 \quad (10)$$

with the abbreviations

$$K_i = 8 + 24\int_0^\infty dx(1 + x)^2[1 - g(x)]$$

$$K_h = -6.44 - \int_0^\infty dx\, F(x)[1 - g(x)]$$

$$F(x) = 12(1 + x) - \frac{15}{8}(1 + x)^{-2} + \frac{27}{64}(1 + x)^{-4} + \frac{75}{64}(1 + x)^{-5}$$

ϕ is the volume fraction of the micelles in solution.

The restriction of the dilute gas approximation, which is the first term of the expansion[19,22]

$$g(r) = \exp\left(-\frac{V(r)}{k_B T}\right)\{1 + n y_1(r) + n^2 y_2(r) + ...\} \quad (11)$$

is little suitable for the evaluation of $g(r)$ in diluted but strongly interacting solutions (y_i are cluster integrals). For the equation of diffusivities (eq 10) Ortega et al.[7] report that they fit the same parameter α for the interaction potential using the well-suited, but difficult HNC approximation[19] without the expansion due to $K_i\phi \ll 1$, or the simple dilute gas approximation with that expansion. We compared the $K_i\phi$ data of Dorshow/Ortega et al.,[1,2,7] on the one hand, with our results, on the other, and could not verify the agreement with the condition $K_i\phi \ll 1$ too. Obviously, there is a mutual cancellation of errors in both approximations, the linear expansion of eq 9 and the restriction of the linear gas part in $g(r)$ (eq 11). Both simplifications are applicable to eq 10 for the apparent diffusion coefficient alone and not for the analysis of apparent molar mass data from eq 9. The used concentrations and so $K_i\phi$ are too large so that a restriction to a linear expansion in eq 9 is not possible. Moreover, the expression for the apparent molar mass without expansion due to $K_i\phi \ll 1$ is not suitable in the simple form for the dilute gas approximation in the limit of small ionic strength.[22] For that reason the theory mentioned above is only processed in the case of diffusion coefficients. But a simple polynominal fit of a suitable order for the inverse molar masses should have the ability to provide the intersection $1/M_0$ in eq 9.

Now the DLVO potential is explained.[20] Using eq 8 the two parts of the potential, V_{attr} and V_{rep}, can be set as an attractive van der Waals and a repulsive electrostatic Debye contribution, respectively. For the case of $\kappa a < 3$ (low screening; see Figure 38 of ref 20 or the discussion in ref 4) it is

$$V_{DLVO}(x) = V_{es}(x) + V_{vdW}(x) \quad (12)$$

$$V_{es}(x) = \psi_0^2 \epsilon a\frac{e^{-2\kappa a x}}{2(1 + x)}\gamma \quad (13)$$

$$V_{vdW}(x) = -\frac{A}{12}\left\{(x^2 + 2x)^{-1} + (x^2 + 2x + 1)^{-1} + 2\ln\left[\frac{x^2 + 2x}{x^2 + 2x + 1}\right]\right\} \quad (14)$$

$$\psi_0 = \frac{\tilde{n}\alpha e}{\epsilon a(1 + \kappa a)}f \qquad \kappa = \sqrt{\frac{8\pi N_A e^2 I}{10^3 \epsilon k_B T}} \quad (15,16)$$

$$I = \mathrm{cmc} + c_{NaCl} + \frac{\alpha}{2}(c - \mathrm{cmc}) \quad (17)$$

ϵ is the dielectric constant of water, ψ_0 the particle surface potential, κ the inverse Debye−Huckel length, I the ionic strength, $\tilde{n}$ the micelle aggregation number, e the electronic charge, N_A Avogadro's number, A the Hamaker coefficient, cmc the critical micelle concentration, c_{NaCl} the added salt concentration, and α the degree of ionization of the micellar surface. γ and f are complicated functions taken from the original monograph (see page 149f of ref 20). We checked the upper limit κa in our case; it is always less than 3. Both integrals in K_i and K_h cannot be solved without a lower cutoff $x_L > 0$ because the attractive part of the potential diverges. The generally accepted value $x_L = 0.04$, which corresponds to the expected Stern layer thickness, has been used.[1,2,4]

The final unknown parameters for our least-squares fitting procedure are the diffusion coefficients D_{0i}, the Hamaker

constant A, and the degree of ionization α. The subscript i denotes various sample environments in connection with the different NaCl concentrations. As the functional dependence of the described theory has only one value for the slope of the curve, it is impossible to fit all three parameters in one step. The curve with the weakest screening (0.03 M NaCl in our case, denoted by 1) is mainly influenced by the repulsive part of the potential and thus by α. Following Dorshow et al.,[1,2] the first fitting step of the program varies only α and D_{01}. A_1 is first an arbitrary constant number. Next, this value of α is adopted as a constant; we take the most screening curve (0.2 M NaCl in our case, denoted by 5) which is mainly influenced by the attractive part of the potential and fit $A = A_5$ and D_{05}. In the next step a new constant value for the Hamaker coefficient using the relation $A_1 = (M_{01}/M_{05})^2 A_5$[23] is calculated, and the procedure is started all over again. This procedure is repeated until self-consistency is obtained. The intermediate curves (0.05 M NaCl, 0.075 M NaCl, and 0.1 M NaCl) are fitted with the derived α and the appropriate value for $A_i = (M_{0i}/M_{05})^2 A_5$ only by a variation from D_{0i}. This theory and procedure are based on three physical and chemical assumptions about the micellar system:

(i) The degree of ionization α is the same for all NaCl concentrations.

(ii) The degree of ionization is the same for all NaGDC concentrations. Oswald's law of dilution is negligible because of the restricted range of concentration.

(iii) The micelles do not grow when the NaGDC concentration is increased. But they grow when the NaCl concentration is increased, and Hamaker's constant depends on the micellar mass.

Experiment

Materials and Preparation. For our measurements the dihydroxy bile salt glycodeoxycholic sodium salt (NaGDC), shown in Figure 1, is used. This bile salt was purchased from Sigma Aldrich. We have checked the sample purity with mass spectrometry and could not find any impurities aside from water. The samples for light scattering were prepared as follows: Different NaCl solutions (NaCl from Fluka, impurities less than 0.1%) in the range 0.03−0.5 M NaCl content were dissolved in bidistilled water. Five different amounts of bile salt were weighed into 25 mL bottles and dissolved in the NaCl solutions. The samples were filtered through a 0.2 μm pore size filter into dust-cleaned sample cells. The cylindrical sample cells are made of quartz glass and have a diameter of 20 mm.

The light scattering experiments were carried out with a commercial SOFICA instrument in the case of static light scattering and an ALV Langen light scattering goniometer in the case of dynamic measurements.

Data Acquisition: Static Light Scattering. The apparent molar mass has been deduced from the Rayleigh ratio at an angle of 90° ($R_{90°}$), which is mainly the scattered intensity of the solution at this angle, $I_{solution}$, which has been corrected in a usual way by subtracting the scattering intensity of the solvent, $I_{solvent}$, and dividing by the primary intensity I_0.

$$R_{90°} = \frac{I_{solution}(90°) - I_{solvent}(90°)}{I_0} \tag{18}$$

Each intensity has been related to the known intensity of toluene as a standard. Finally, the quantity

$$\frac{K(c - \mathrm{cmc})}{R_{90°}} = \frac{1}{M_{app}} \qquad K = \frac{4\pi^2 {n_0}^2}{\lambda^4 N_A}\left(\frac{\partial n}{\partial c}\right)^2 \tag{19}$$

was taken, where K is the Rayleigh factor, n_0 the refractive index of the solute, $\lambda = 632.8$ nm the laser wave length, and $\partial n/\partial c$ the refractive index increment, which has been deduced with an Abbe refractometer. Experimental accuracies for the quantity M_{app} were in the range of ±5%. The angular independence has been checked for each sample, measuring the scattered intensity at 10 different angles in the range from 45° to 120°. The angular corrected intensity was nearly the same for all detector positions. The values from Kratohvil and Dellicolli have been taken for the critical micelle concentration.[24]

Data Acquisition: Dynamic Light Scattering. The apparent diffusion coefficient has been deduced from a second-order cumulant analysis (eq 21) from the normalized field autocorrelation function $g_1(\tau)$, which has been derived from the intensity autocorrelation function $g_2(\tau)$ via Siegerts relation (eq 20).[25,26]

$$g_2(\tau) = \frac{\overline{I(t)\, I(t+\tau)}}{I^2(t)} = 1 + B{g_1}^2(\tau) \tag{20}$$

$$\ln g_1(\tau) = -q^2 D_{app}\tau + \frac{\mu_2}{2}\tau^2 \tag{21}$$

B is an instrument factor and μ_2 the so-called second cumulant. The correlation function measurements were made at a scattering angle of 45°, but 532 nm wavelength light was used, and the autocorrelation function of the intensity fluctuations was taken using a ALV 5000 E multiple-τ digital autocorrelator. Experimental errors for the quantity D_{app} are in the range of ±3%.

Results and Discussion

First, the molar masses of the micelles at different NaCl concentrations and various temperatures have been calculated (summarized in Table 1), by fitting the curves of $1/M_{app}$ versus $(c - \mathrm{cmc})$ by a simple second-order least-squares fit and taking the intersections as $1/M_0$. Figure 2 shows a corresponding plot for the inverse micellar masses at 25 °C. The other three plots look similar, and therefore their representation is skipped.

Next, the values M_{0i} and $\tilde{n}_i = M_{0i}/471.6$ (471.6 g/mol is the molar mass of the bile salt) have been taken in order to determine the volume fraction ϕ of each sample from eq 22,

$$\phi = \frac{4\pi a^3}{3}\frac{N_A(c - \mathrm{cmc})}{1000 M_{0i}} \tag{22}$$

ψ_0 from eq 15 and A_i to fit the apparent micellar diffusivities as explained in the section above (Table 1). For each variation of D_{0i} and α the variable parameters such as a, ϕ, and κ need to be recalculated. Two representative plots for 20 and 35 °C are printed in Figure 3a and b, respectively.

The excellent agreement between experimental data and the fitted theoretical curves should be noted. Remarkable is the good agreement between experiment and calculation of the three intermediated curves, which is only achievable by using an attractive part of the potential (eqs 8, 12, 14). It is important to note that the percentage increase for the molar masses (Figure 2) is stronger than the increase for the diffusivities (Figure 3) as expected because of the additional negative factor K_h in eq 10. This is a confirmation of the used hydrodynamic interaction theory. The slightly downward curvature of the lines of lower

TABLE 1: Investigated Micellar Parameters Molar Mass M_0, Aggregation Number $\tilde{n}$, Diffusion Coefficient D_0, Hydrodynamic Radius a, and the Degree of Ionization α, Sorted by Temperature and NaCl Content in Solution

T [°C]	α	c_{NaCl} [mol/L]	M_0 [g/mol]	$\tilde{n}$	$D_0 \times 10^8$ [cm²/s]	a [nm]
20	0.368	0.03	5496	11.6	153.831	1.39
		0.05	6992	14.8	137.74	1.55
		0.075	7381	15.6	127.415	1.68
		0.1	8189	17.4	120.035	1.78
		0.2	11346	24.1	102.5	2.08
25	0.382	0.03	5217	11.1	176.868	1.38
		0.05	6097	12.9	160.58	1.52
		0.075	6865	14.6	147.395	1.66
		0.1	8152	17.3	139.054	1.75
		0.2	10618	22.5	119.015	2.05
30	0.39	0.03	5065	10.7	202.317	1.38
		0.05	5925	12.6	184.991	1.50
		0.075	6642	14.1	169.195	1.64
		0.1	7457	15.8	161.032	1.73
		0.2	10481	22.2	139.955	1.99
35	0.398	0.03	4858	10.3	229.139	1.38
		0.05	5671	12	209.629	1.51
		0.075	6152	13	193.437	1.63
		0.1	7174	15.2	183.087	1.72
		0.2	9900	21	158.167	2.00

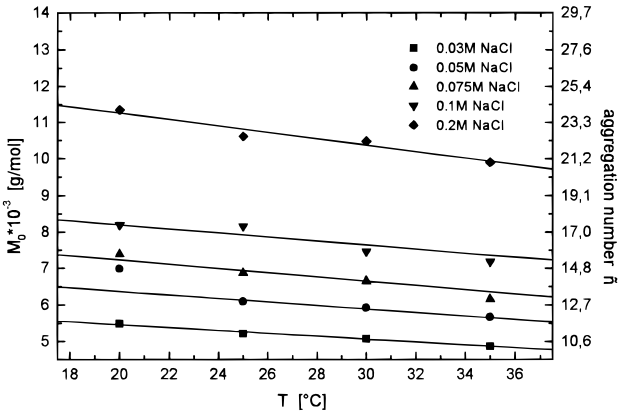

Figure 4. Temperature dependence of the molar masses and aggregation numbers for different NACl solutions. The aggregation number is $\tilde{n} = M_0/471.6$. The lines are linear least-squares fits.

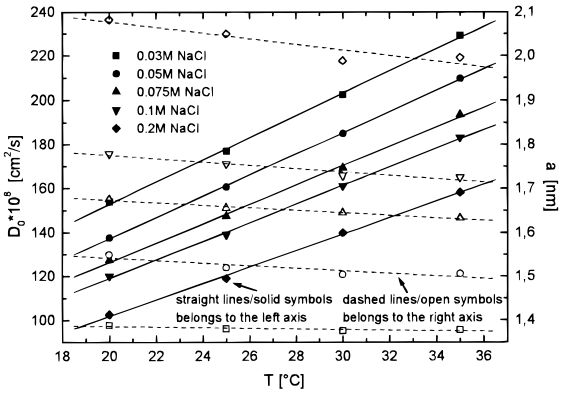

Figure 5. Temperature dependence of the diffusion coefficients and the hydrodynamic radii for different NaCl solutions. The hydrodynamic radii are calculated with the equation $a = (k_B T)/(6\pi\eta(T)D_0)$. The lines are linear least-squares fits.

NaCl content is due to the dependence of D_{app} on the ionic strength (eqs 10−14).

The values for M_0, $\tilde{n}$, and a slightly decrease whereas D_0 and α increase when the temperature is increased (Figures 4−6 and Table 1). The Hamaker coefficient A does not show a remarkable dependence on temperature. Because of the divergence of the van der Waals potential for values of $x \rightarrow 0$ and the restriction of the cutoff length x_L, the derived absolute values of A are rather meaningless, as they strongly depend on the lower cutoff x_L. The value of α is almost insensitive to x_L. We checked the fitting routine with $x_L = 0.02$ and 0.08: α varies within ±2%.

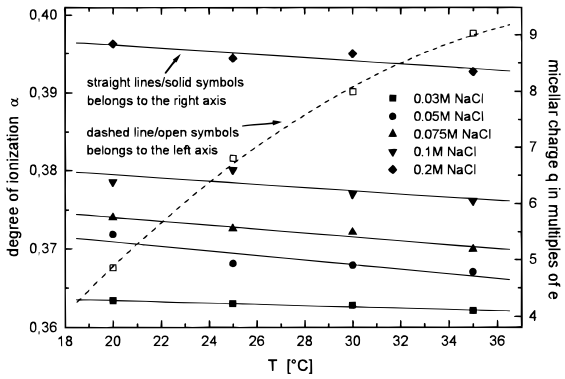

Figure 6. Temperature dependence of the degree of ionization and the overall micellar charge for different NaCl solutions. The micellar charge q is calculated with the equation $q = \tilde{n}\alpha$. The lines are least-squares fits to guide the eyes.

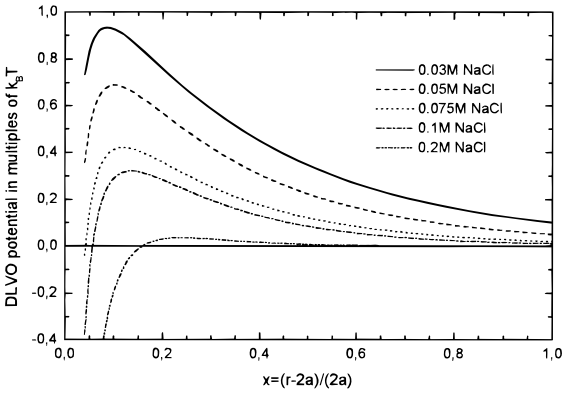

Figure 7. Derived DLVO potential between two micelles at 35 °C for different NaCl solutions.

Figure 6 shows that although the degree of ionization increases monotonically with temperature, the total charge of the micelles decreases because the aggregation number is reduced. To verify the fitted data, the calculated values q/a have been checked with some electrophoretic measurements at 25 °C. The agreement is in the range of ±10%, and the behavior is the same: q/a decreases with temperature.

Figure 7 shows the DLVO potential derived with the fitted values at 35 °C from Table 1 which acts between two micelles in different NaCl solutions. The repulsive part decreases with increased screening until the rampart of the potential has nearly disappeared. For solutions of higher ionic strength (>0.2 M NaCl) where the potential is only attractive a particle coagulation process is expected. For that reason our described interaction theory supports models for the high-salt region, too, which take growth processes into account. The micellar growth behavior of bile salt systems in the region of high ionic strength is well discussed by the primary-secondary-micelle theory from Mazer et al.[8,9] Unfortunately, there is no continuous transition from the hypothesis supposed in this paper and the primary-secondary-micelle theory. All calculated potentials from curves of $1/M_{app}$ or D_{app} with negative slopes can only be attractive. Therefore, stable systems with coagulation processes in the sense of our theory cannot exist.

Summary

We have discussed a self-consistent fit program for dynamic light scattering data on more complex surfactants which have a growth behavior with the increase of added salt concentration in the low-salt region, too. Some micellar parameters of the bile salt NaGDC are derived, and the interaction potential between two micelles according to the DLVO theory is estimated. The agreement between theory and the experimental data is excellent. Based on the previously documented analysis from Dorshow et al.,[1,2] the expanded fit procedure confirms the validation of the theory and assumptions. Without taking into account micellar growth with the increase of surfactant content, the concentration dependence of the measured quantities was explained.

Acknowledgment. The authors are indebted to Maria Schwarz for helpful discussions and support with the electrophoretic measurement. We give many thanks to Sebastian Janich for critically reading the manuscript. This work was supported by the Deutsche Forschungsgemeinschaft.

References and Notes

(1) Dorshow, R.; Briggs, J.; Bunton, C. A.; Nicoli, D. F. *J. Phys. Chem.* **1982**, *86*, 2388.

(2) Dorshow, R. B.; Bunton, C. A.; Nicoli, D. F. *J. Phys. Chem.* **1983**, *87*, 1409.

(3) Degiorgio, V.; Corti, M. *Physics of Amphiphiles: Micelles, Vesicles and Microemulsions*; Elsevier: Amsterdam, 1985.

(4) Corti, M.; Degiorgio, V. *J. Phys. Chem.* **1981**, *85*, 711.

(5) Missel, P. J.; Mazer, N. A.; Benedek, G. B.; Young, C. Y.; Carey, M. C. *J. Phys. Chem.* **1980**, *84*, 1044.

(6) Ikeda, S.; Hayashi, S.; Imae, T. *J. Phys. Chem.* **1981**, *85*, 106.

(7) Ortega, F.; Bacaloglu, R.; McKenzie, D. C.; Bunton, C. A.; Nicoli, D. F. *J. Phys. Chem. Lett.* **1990**, *94/2*, 501.

(8) Mazer, N. A.; Carey, M. C.; Kwasnick, R. F.; Benedek, G. B. *Biochemistry* **1979**, *18*, 3064.

(9) Schurtenberger, P.; Mazer, N.; Känzig, W. *J. Phys. Chem.* **1983**, *87*, 308.

(10) Hjelm, R. P.; Thiyagarajan, P.; Alkan-Onyuksel, H. *J. Phys. Chem.* **1992**, *96*, 8653.

(11) Egelhaaf, S. U.; Schurtenberger, P. *J. Phys. Chem.* **1994**, *98*, 8560.

(12) Schwarz, M. Ph.D. Thesis, Martin-Luther-Universität Halle, Halle (Saale), Germany, 1998.

(13) Bendedouch, D.; Chen, S.-H.; Koehler, W. C. *J. Phys. Chem.* **1983**, *87*, 2621.

(14) Berr, S. S.; Caponetti, E.; Johnson, J. S.; Jones, R. R. M.; Magid, L. J. *J. Phys. Chem.* **1986**, *90*, 5766.

(15) Porte, G.; Appell, J. *J. Phys. Chem.* **1981**, *85*, 2511.

(16) Berne, B. J.; Pecora, R. *Dynamic Light Scattering*; Wiley: New York, 1976.

(17) Small, D. M. The physical chemistry of the cholanic acids. In *The Bile Acids*; Nair, P. P., Kritchevsky, D., Eds.; Plenum Press: New York, 1971.

(18) Pusey, P. N.; Tough, R. J. A. In *Dynamic Light Scattering: Applications of Photon Correlation Spectroscopy*; Pecora, R., Ed.; Plenum: New York, 1985.

(19) Balescu, R. *Equilibrium and Nonequilibrium Statistical Mechanics*; Krieger Publishing Co.: Malabar, FL, 1991.

(20) Verwey, E. J. W.; Overbeek, J. T. G. *Theory of the Stability of Lyophobic Colloids*; Elsevier: New York, 1948.

(21) Felderhof, B. U. *J. Phys. A: Math. Gen.* **1978**, *11*, 929.

(22) Neal, D. G.; Purich, D.; Cannell, D. S. *J. Chem. Phys.* **1984**, *80* (7), 3469.

(23) Sonntag, H.; Strenge, K. *Coagulation Kinetics and Structure Formation*; Deutscher Verlag der Wissenschaften: Berlin, 1987.

(24) Kratohvil, J. P.; Dellicolli, H. T. *Can. J. Biochem.* **1968**, *46*, 945.

(25) Koppel, D. E. *J. Chem. Phys.* **1972**, *57*, 4814.

(26) Siegert, A. J. F. *MIT Rad. Lab. Rep. No. 465*, 1943.